

Permanent electric dipoles in $B^1\Pi$ and $D^1\Pi$ states of NaRb: Experiment and theory

O. Nikolayeva, I. Klincare, M. Auzinsh, M. Tamanis, and R. Ferber
Department of Physics, University of Latvia, Riga LV-1586, Latvia

E. A. Pazyuk, A. V. Stolyarov, and A. Zaitsevskii
Department of Chemistry, Moscow State University, Moscow 119899, Russia

R. Cimraglia
Dipartimento di Chimica, Università di Ferrara, Via Borsari 46, I-44100, Ferrara, Italy

(Received 26 April 2000; accepted 27 June 2000)

The paper presents experimentally obtained permanent electric dipole moment values (μ) in electronically excited $B^1\Pi$ and $D^1\Pi$ states of $^{23}\text{Na}^{85}\text{Rb}$ and $^{23}\text{Na}^{87}\text{Rb}$ isotopomer molecules for a number of vibrational and rotational levels (v', J'). The method is based on measuring relative intensities of “forbidden” fluorescence lines appearing due to dc Stark effect induced e/f parity mixing for a particular (v', J')-level, combined with electric radio frequency–optical double resonance measurement of Λ -splitting energy $\Delta_{e,f}$. The measured $D^1\Pi$ state μ values are close to 6 D, representing minor changes with the vibrational level v' varying from 0 to 12 and J' in the region between 7 and 50, while the measured $B^1\Pi$ state μ values are about 3 D for $v'=4, 5$ and 6. The $X^1\Sigma^+$, $B^1\Pi$, and $D^1\Pi$ dipole moment functions $\mu(R)$ are calculated *ab initio* using the many body multipartitioning perturbation theory for explicit treatment of core-valence correlations. The theoretical and experimental dipole moment estimates are in a perfect agreement for the ground state and the $D^1\Pi$ state, differing by 15%–25% for the $B^1\Pi$ state. © 2000 American Institute of Physics. [S0021-9606(00)00336-6]

I. INTRODUCTION

The permanent electric dipole moment of an electronically excited molecular state carries valuable information on its electronic structure as well as on energy transfer properties. As has been demonstrated by our recent studies^{1,2} on the NaK molecule, which is up to now the best-understood heteronuclear alkali dimer, it is possible to obtain reliable permanent electric dipole moment values for given v' and J' levels belonging to the excited $^1\Pi$ states by measuring dc Stark effect induced changes in laser induced fluorescence (LIF) spectra combined with the direct determination of e/f Λ -splitting frequency ($\Delta_{e,f}$) of the (v', J')-level under study by applying the electric Radio Frequency–Optical Double Resonance (RF–ODR) method. On the other hand, the *ab initio* calculation based on the multipartitioning perturbation theory (MPPT) demonstrated excellent agreement with experimentally obtained permanent dipole values of the $D^1\Pi$ state.¹ The NaK data on permanent electric dipoles are the only ones existing for electronically excited heteronuclear alkali dimers, the objects that are now of increased interest because of studies of collision dynamics and photoassociative spectra, laser cooled and trapped alkaline atoms. As follows from the present state of research, mixed alkali diatomics, such as NaK, NaRb, and KRb seem to be promising for the formation of ultracold molecules.^{3,4}

The main purpose of the present work is to use the methods of measurement and *ab initio* calculations of permanent electric dipole moments, developed and approved for NaK in Ref. 1 and 2, to study the NaRb molecule. The NaRb molecule has been recently intensively studied spectroscopically

by the Katô group.^{5–9} However, the existing spectroscopic information on NaRb is much scarcer than for NaK. Only the $X^1\Sigma^+$ and $B^1\Pi$ electronic states have been studied systematically by high resolution methods of polarization spectroscopy and optical-optical double resonance spectroscopy.^{6–9} The dense perturbation pattern discovered in the $B^1\Pi$ state was ascribed to interaction with perturbing $b^3\Pi$ and $c^3\Sigma^+$ triplet states correlating to the same atomic limit Na ($3s$) + Rb ($5p$). As far as molecular terms correlating to the Na ($3p$) + Rb ($5s$) atoms are concerned, only the $D^1\Pi$ state has been studied⁵ using LIF methods, namely, by exciting selectively the $D^1\Pi$ (v', J')-levels with the fixed frequency Ar⁺-laser lines and analyzing spectrally resolved $D^1\Pi(v', J') \rightarrow X^1\Sigma^+(v'', J'')$ LIF progressions. The difficulties in working on NaRb arise from the presence of two isotopomer mixture $^{23}\text{Na}^{85}\text{Rb}$ and $^{23}\text{Na}^{87}\text{Rb}$ and more dense rotational pattern than in NaK, as well as from the stronger spin-orbit interaction leading to more pronounced perturbations due to the role of Rb atom.¹⁰

We report the first experimental data on permanent electric dipole moments for a number of (v', J')-levels belonging to the $B^1\Pi$ and $D^1\Pi$ states of $^{23}\text{Na}^{85}\text{Rb}$ and $^{23}\text{Na}^{87}\text{Rb}$ molecules, as well as the corresponding results of *ab initio* MPPT calculations. The employed computational procedure is based on direct perturbative construction of one-electron density matrix avoiding somewhat burdensome finite-field technique of Ref. 1. Neither experimental nor theoretical data on the NaRb excited states permanent dipoles can be found in literature. The only measurement was performed for the ground $X^1\Sigma^+$ state by molecular beam deflection method yielding electric dipole moment value 3.1 ± 0.3 D.¹¹

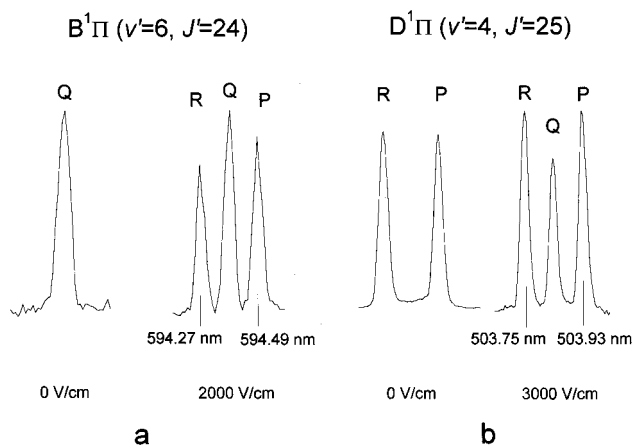


FIG. 1. Fragments of NaRb LIF spectra demonstrating appearance of extra lines induced by dc Stark effect in the $B^1\Pi(6,24) \rightarrow X^1\Sigma^+(0,24)$ transition following Q -type excitation (a) and in the $D^1\Pi(4,25) \rightarrow X^1\Sigma^+(1,24)$ and $26)$ transitions following R -type excitation (b).

II. EXPERIMENT

A. Method

The procedure of experimental determining of the permanent electric dipole moment values μ for the Π -state (v', J')-levels, which is described in more details in Ref. 1, consists of two steps.

First, after selecting and identifying a definite LIF $^1\Pi \rightarrow X^1\Sigma^+$ progression consisting of either singlets (following the Q -excitation) or doublets (following the P - or R -excitation), a dc electric field \mathcal{E} is applied to achieve $e-f$ parity mixing between the Λ -doublet components of the $^1\Pi$ state. As a result, extra lines appear in the LIF spectrum, namely P - and R -lines following Q -excitation or Q -lines following P - or R -excitation, when the Stark energy $W_{el} = -\mu\mathcal{E}$ becomes comparable to Λ -splitting $\Delta_{e,f}$.¹² Thus, the LIF spectra are transformed from Q -singlets or (P, R)-doublets to the (P, Q, R)-triplets, see Fig. 1. The ratio I_f/I_a of extra ("forbidden") line intensity I_f over the "allowed" line intensity I_a is governed by the absolute value of parameter $\mu\mathcal{E}/\Delta_{e,f}$, thus, fitting the I_f/I_a as dependent on \mathcal{E} , see Fig. 2, will yield an absolute value of the $\mu/\Delta_{e,f}$ ratio. Some details on simulation of \mathcal{E} -dependence of I_f/I_a and fitting routine used to obtain the $\mu/\Delta_{e,f}$ ratio, including the treatment for different polarization and geometry, as well as discussion of possible sources of errors, can be found in Refs. 1 and 2.

At the second step the absolute value of the Λ -splitting energy $\Delta_{e,f}$ is measured directly by the electric RF-ODR method, the essence of which is the following.¹³⁻¹⁵ Position of a "forbidden" line of the LIF progression under study is singled out with the monochromator in the presence of a dc external electric field, see Fig. 1. Then, instead of the dc electric field, the frequency scanned RF electric field is applied to the Stark plates. When frequency f hits the resonance condition $hf = \Delta_{e,f}$, forbidden line I_f is observed at its maximum intensity. The resonance signal $I_f(f)$, see Fig. 3, in the simplest case is of the Lorentzian shape.¹⁴ Knowing the Λ -splitting value $\Delta_{e,f}$, one may pass from the $\mu/\Delta_{e,f}$ ratio

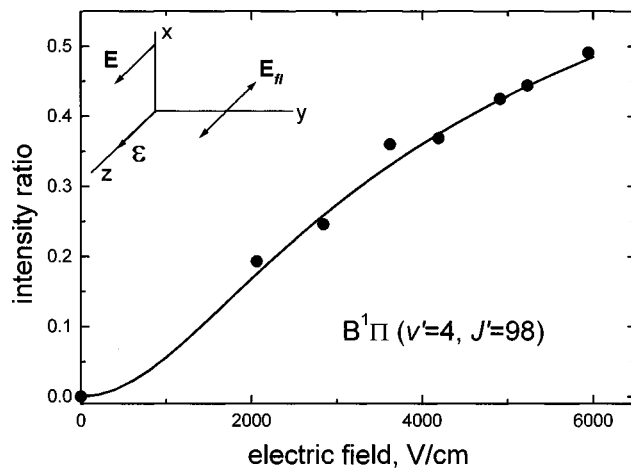


FIG. 2. Experimentally obtained intensity ratios I_f/I_a for LIF originating from $^{23}\text{Na}^{85}\text{Rb } B^1\Pi(4,98)$ level versus applied dc electric field \mathcal{E} . \mathbf{E}, \mathbf{E}_f denote exciting light and fluorescence light vectors, respectively. Fitting procedure yields $\Delta_{e,f}/\mu = 6.06 \times 10^{-4} \text{ cm}^{-1}/\text{D}$.

to the absolute value of the permanent electric dipole moment μ for a particular v', J' level belonging to the $^1\Pi$ electronic state.

B. Experimental setup

The experimental setup and equipment used is similar to that employed in our previous NaK studies.^{1,2,15} Briefly, the $^{23}\text{Na}^{85}\text{Rb}$ and $^{23}\text{Na}^{87}\text{Rb}$ molecules were formed from a mixture of rubidium and sodium metal, approximately 4:1 (by weight), in an alkali-resistant glass cell at the temperature $T \approx 550 \text{ K}$. The natural abundance of ^{85}Rb and ^{87}Rb isotopes is about 72.2% and 27.8%, respectively. The cell contained Stark plates made of carefully polished stainless steel $\sim 6.5 \text{ mm}$ in diameter with the spacing about 1.0 mm measured with $\approx 3\%$ accuracy. The exciting laser beam was directed through the gap between the Stark plates. The fluorescence zone was imaged onto the entrance slit of a double-monochromator with two 1200 groves/mm gratings provid-

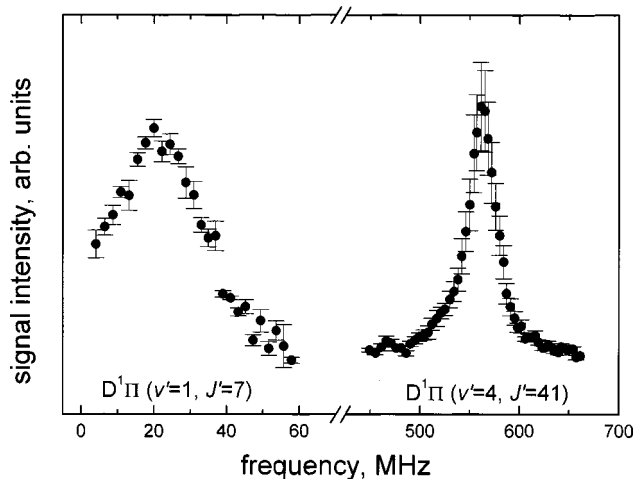


FIG. 3. Examples of experimentally obtained RF-ODR signals for $D^1\Pi$ state of $^{23}\text{Na}^{85}\text{Rb}$.

TABLE I. Exciting laser wavelengths (λ_{exc}) measured $e-f$ splittings ($|\Delta_{ef}|$), and permanent electric dipole moments obtained from the experiment ($|\mu_{\text{exp}}|$) and calculated by MPPT (μ_{calc}). Positive μ -values correspond to Na^-Rb^+ polarity.

Isotopomer	$(v'', J'') \rightarrow (v', J')$	λ_{exc} , (nm)	$ \Delta_{ef} $ (MHz)	$ \mu_{\text{exp}} $ (D)	μ_{calc} (D)
$B^1\Pi$ state					
$^{23}\text{Na}^{85}\text{Rb}$	(11,97 \rightarrow 4,98)	647.1	68 \pm 3	3.5 \pm 0.3	-2.7
$^{23}\text{Na}^{85}\text{Rb}$	(7,115 \rightarrow 5,116)	632.8	220 \pm 5	3.1 \pm 0.2	-2.6
$^{23}\text{Na}^{87}\text{Rb}$	(10,24 \rightarrow 6,24)	632.8	52 \pm 5	3.0 \pm 0.4	-2.6
$D^1\Pi$ state					
$^{23}\text{Na}^{85}\text{Rb}$	(2,44 \rightarrow 0,44)	514.5	576.5 \pm 2	6.0 \pm 0.4	+6.2
$^{23}\text{Na}^{85}\text{Rb}$	(3,8 \rightarrow 1,7)	514.5	20 \pm 2	6.7 \pm 1.0	+6.1
$^{23}\text{Na}^{85}\text{Rb}$	(5,24 \rightarrow 4,25)	514.5	210 \pm 5	6.2 \pm 0.5	+6.1
$^{23}\text{Na}^{85}\text{Rb}$	(0,41 \rightarrow 4,41)	501.7	561 \pm 1	5.6 \pm 0.4	+6.1
$^{23}\text{Na}^{87}\text{Rb}$	(6,45 \rightarrow 6,44)	514.5	671 \pm 2	6.2 \pm 0.4	+6.1
$^{23}\text{Na}^{87}\text{Rb}$	(2,35 \rightarrow 10,36)	496.5	726 \pm 1	6.1 \pm 0.4	+6.0
$^{23}\text{Na}^{85}\text{Rb}$	(3,49 \rightarrow 12,50)	496.5	834.5 \pm 1	5.8 \pm 0.5	+5.9

ing reciprocal dispersion of 5 $\text{\AA}/\text{mm}$ and spectral resolution of ≈ 0.2 \AA . Calibration of LIF spectra by neon and argon discharge lines allowed to achieve an absolute spectral accuracy of about 0.1 \AA . We used fixed frequency lines from Spectra Physics 171 Ar^+ laser, as well as from Kr^+ and He-Ne lasers, see Table I, to excite a particular (v', J') -level belonging to the $D^1\Pi$ and $B^1\Pi$ states of NaRb. To maintain the conditions of simultaneous excitation of e and f parity components, we preferred to employ the multi-mode laser operation, with typical laser line contour widths ≈ 10 GHz for Ar^+ or Kr^+ lasers and ≈ 1.2 GHz for the He-Ne laser. In some cases we were forced to employ the single-mode regime to simplify the LIF spectra. The RF field for the RF-ODR measurements was produced by Mini-circuit voltage controlled oscillators covering the frequency region 5–900 MHz followed by an amplifier Mini-circuit ZHL-2-12 to obtain RF field amplitude value up to 5 V, as well as by Wavetek generator covering the 1–60 MHz region.

III. EXPERIMENTAL RESULTS

Examples of Stark effect induced changes in LIF spectra and corresponding fits of the I_f/I_a signal are shown in Figs. 1 and 2, while some typical electric RF-ODR signals are presented in Fig. 3. Experimental values of the Δ_{ef} splitting are presented in Table I. The permanent electric dipole moments $\mu(v', J')$, which are obtained by combining Δ_{ef} values with the Δ_{ef}/μ ratios resulted from the fitting of signals as given in Fig. 2, are depicted in Fig. 4 and presented in Table I for all studied (v', J') -levels of the $B^1\Pi$ and $D^1\Pi$ states. The permanent electric dipole moment error in Table I accounts for the inaccuracies in Δ_{ef} values and in determining the gap between the Stark plates, as well as for the discrepancies of μ -values obtained in different experiments.

A few notes ought to be made concerning the v', J' assignment. Unambiguous vibrational assignment has been achieved from the vibrational spacings in LIF progressions and by comparison of the experimental LIF intensity distribution with the simulated Franck-Condon factors.

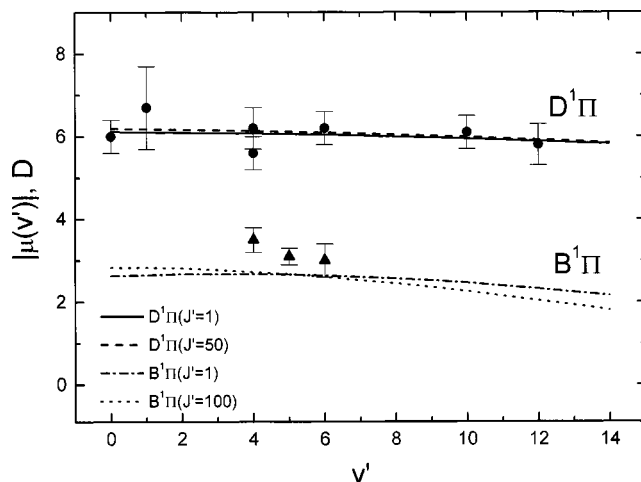


FIG. 4. Absolute values of electric dipole moments $|\mu(v')|$ for the $D^1\Pi$ (circles) and $B^1\Pi$ (triangles) states of NaRb as functions of vibrational quantum number v' . The respective J' values can be found in Table I. The smooth lines represent $|\mu(v')|$ obtained from *ab initio* MPPT calculations for $J'=1$ and 100 ($B^1\Pi$ state), as well as for $J'=1$ and 50 ($D^1\Pi$ state).

As it appeared, rotational and isotope assignments of the LIF spectra progressions were neither easy, nor unambiguous. As a tentative guide we used the data given in Table II of Ref. 5, where a number of (v', J') -levels of $B^1\Pi$ and $D^1\Pi$ states excited by Kr^+ , He-Ne, and Ar^+ laser lines is presented. However, the J' values are not always given there and the particular isotopomer is not defined. Besides, we have observed several progressions not mentioned in Ref. 5. To identify the LIF progressions originating from a definite $B^1\Pi$ state (v', J') -level, we used spectroscopic constants for the $B^1\Pi$ state from Refs. 6 and 7 and for the $X^1\Sigma^+$ state from Refs. 6 and 9. As far as the $B^1\Pi$ state level with $v'=6$ excited by a Q -transition is concerned, we managed to assign unambiguously the value $J'=24$ for the $^{23}\text{Na}^{87}\text{Rb}$ isotopomer, see Table I, by the following routine. First, we measured the rotational spacing between P , Q , and R lines in presence of an external dc electric field, which yielded $J'=23\pm 1$. The least deviation of 0.002 cm^{-1} between the $B^1\Pi(v'=6, J') \rightarrow X^1\Sigma^+(v''=10, J'')$ transition frequencies calculated using molecular constants from Refs. 6 and 9 and the exciting laser frequency was obtained for $J'=22$ of $^{23}\text{Na}^{85}\text{Rb}$ and for $J'=24$ of $^{23}\text{Na}^{87}\text{Rb}$. In order to decide between these possibilities, we checked the deviation $\Delta\nu$ between the measured (ν_{exp}) and calculated (ν_{calc}) line positions for the LIF v' -progression $B^1\Pi(v'=6, J') \rightarrow X^1\Sigma^+(v'', J'')$. As it revealed, only in the case of $J'=24$ for the $^{23}\text{Na}^{87}\text{Rb}$ isotopomer the deviation is within limits of the experimental errors. The high $J' \approx 100$ values of the $B^1\Pi$ state given in Table I are less reliable because of less accuracy of the molecular constants in Refs. 6 and 9 for high J' . It also means that the isotopomer is not determined unambiguously for these transitions since the respective procedures are mutually interrelated. Similar situation takes place in the $D^1\Pi$ state, see Table I, in which we suppose that the data for smaller J' values are more reliable, the possible inaccuracy of J' not exceeding ± 1 . It has to be noted that the set of $D^1\Pi$ state molecular constants in Ref. 5

is rather scarce; it does not allow to reproduce the term energies accurately enough, leading up to several wave numbers deviation from the excitation energy. However, the possible inaccuracy in J' values practically does not affect the dipole moment values presented in Table I.

IV. *Ab initio* DIPOLE MOMENT CALCULATIONS

The *ab initio* electronic structure calculations of NaRb were performed by means of the many-body multipartitioning perturbation theory (MPPT). This approach implies the perturbative construction of a state-selective effective Hamiltonian \tilde{H} within the model space spanned by an appropriate set of Slater determinants $\{|J\rangle\}$, using several quasi-one-electron zero-order Hamiltonians simultaneously.^{16,17} The second-order MPPT expression for the Hermitian effective Hamiltonian matrix resembles the one which is appearing in the conventional quasidegenerate perturbation theory,¹⁸

$$\begin{aligned} \langle J|\tilde{H}|J'\rangle &= \langle J|H|J'\rangle + \frac{1}{2} \sum_{K: \substack{|\tilde{K}\rangle \in L_p \\ K \neq J, J'}} \langle J|H|K\rangle \\ &\times \left(\frac{1}{\Delta(J' \rightarrow K)} + \frac{1}{\Delta(J \rightarrow K)} \right) \langle K|H|J'\rangle, \quad (1) \end{aligned}$$

where \tilde{H} is the total many-electron Hamiltonian and the energy denominators $\Delta(J \rightarrow K)$ are given by the formula

$$\begin{aligned} \Delta(J \rightarrow K) &= \sum_{r: N_r^K < N_r^J} (N_r^J - N_r^K) \epsilon_r^\oplus \\ &- \sum_{s: N_s^K > N_s^J} (N_s^K - N_s^J) \epsilon_s^\ominus. \quad (2) \end{aligned}$$

Here N_r^J and N_r^K denote the occupancy of the r th spatial orbital in the model space determinant $|J\rangle$ and the outer space determinant $|K\rangle$, respectively. The entities ϵ_r^\oplus , ϵ_s^\ominus are the nonrelaxed orbital ionization potentials and electron affinities with opposite signs, defined with respect to the model-space approximation for the target states. Diagonalization of \tilde{H} provides energy estimates and model wave functions $|\tilde{\psi}_m\rangle$ for all the target states simultaneously.

To extend the MPPT scheme to one-electron property calculations, one can proceed via the evaluation of the (transition) density matrix (cf. Ref. 19). The first-order approximation for the spin-free $m \rightarrow n$ transition density matrix ${}^{mn}\rho$ compatible with the use of the second-order effective Hamiltonian (1) is given by

$$\begin{aligned} {}^{mn}\rho_{rs} &= \langle \tilde{\psi}_m | E_{sr} | \tilde{\psi}_n \rangle + \sum_{J, J'} \langle \tilde{\psi}_m | J \rangle \\ &\times \langle J' | \tilde{\psi}_n \rangle \sum_K \left(\frac{\langle J | E_{sr} | K \rangle \langle K | H | J' \rangle}{\Delta(J' \rightarrow K)} \right. \\ &\left. + \frac{\langle J | H | K \rangle \langle K | E_{sr} | J' \rangle}{\Delta(J \rightarrow K)} \right), \quad (3) \end{aligned}$$

where E_{sr} is the conventional spin-free one-electron excitation operator (unitary group generator) which can be ex-

pressed in terms of the spin-orbital creation/annihilation operators as $E_{sr} = a_{s\alpha}^\dagger a_{r\alpha} + a_{s\beta}^\dagger a_{r\beta}$. The required dipole moment estimates are immediately obtained as $\sum_{rs} {}^{mn}\rho_{rs} D_{sr}$, where $\|D_{sr}\|$ is the electric dipole matrix in the orbital basis. It is worth noting that the procedure described above is strictly equivalent to the MPPT computation of the first-order effective electric dipole operator with subsequent evaluation of its diagonal matrix element for the m th model wave function $|\tilde{\psi}_m\rangle$.

Since summation over the outer space determinants ($|K\rangle$) in Eq. (3) is in fact restricted to single excitations of the model space configurations, the direct perturbative construction of ${}^{mn}\rho_{rs}$ is not expensive and, therefore, offers an attractive alternative to the accurate but rather cumbersome finite-field technique successfully used in our previous studies.^{1,15}

The procedure of MPPT correlation treatment employed in the present work was generally similar to that used in Refs. 15 and 20. In order to incorporate the scalar (spin-independent) relativistic effects into our calculations, we replaced the inner core shells by averaged relativistic pseudopotentials,^{21,22} leaving 9 electrons of each atom for explicit treatment. The atomic Gaussian basis sets (7s7p5d2f)/[6s6p4d2f] Rb, (8s8p5d1f)/[7s6p4d1f] Na were composed of the outer-core and valence pseudopotential-adapted (*sp*) bases,^{21,22} diffuse parts of the ‘‘all-electron’’ bases for electric property calculations,²³ and additional diffuse and polarization functions. The determinants were constructed from the solutions of the state-average SCF problem for two lowest ${}^2\Sigma^+$ electronic states of NaRb⁺. The model space for the MPPT calculations was a full valence CI space, i.e., it comprised all the possible distributions of two valence electrons among the valence and virtual orbitals; therefore, the perturbative corrections corresponded to the core-valence correlation and residual core polarization effects. The completeness of the model space and the separability of energy denominators (2) guaranteed the size consistency of energy and dipole moment estimates.

The *ab initio* permanent electric dipole moment functions $\mu(R)$ for the $X^1\Sigma^+$, $B^1\Pi$, and $D^1\Pi$ states of NaRb are presented in Table II. These functions were converted to the relevant theoretical $\mu_{\text{calc}}(v', J')$ values (Table I, Fig. 4) by means of vibrational wave functions corresponding to the RKR potential curves. The $B^1\Pi$ curve has been derived from the molecular constants given in Ref. 6, while for the $D^1\Pi$ state we used the data from Ref. 5. The ground state μ value with $v''=0$, calculated with the RKR potential from Ref. 6, is 3.3 D, which agrees with the experimental value 3.1 ± 0.3 D.¹¹

V. DISCUSSION

The measured absolute values of permanent electric dipoles for the $D^1\Pi$ state of NaRb for vibrational levels varying from $v'=0$ to $v'=12$ are close to 6 D, demonstrating minor changes with v', J' (see Table I and Fig. 4). The experimental μ values for the NaRb $B^1\Pi$ state are approximately two times smaller, being close to 3 D. As follows from the results presented in Table I, the experimental data

TABLE II. *Ab initio* permanent electric dipole moment values μ for the $X^1\Sigma^+$, $B^1\Pi$, and $D^1\Pi$ states of NaRb as functions of the internuclear distance R . Positive μ -values correspond to Na^-Rb^+ polarity.

R (a.u.)	$X^1\Sigma^+$	$d(R)$ (D)	
		$B^1\Pi$	$D^1\Pi$
5.4	2.949	0.469	-1.060
5.9	3.063	-0.134	0.349
6.4	3.204	-0.781	1.821
6.885 ^a	3.337	-1.419	3.289
7.4	3.448	-2.076	4.734
7.8928 ^b	3.501	-2.615	5.938
8.4	3.463	-2.962	6.786
8.9	3.329	-3.053	7.148
9.4	3.086	-2.878	7.077
9.9	2.750	-2.554	6.644
10.4	2.349	-2.174	5.874
10.9	1.928	-1.787	4.973
11.5	1.458	-1.389	3.903
12.1	1.058	-1.059	2.955
12.65	0.768	-0.816	2.214
13.25	0.532	-0.629	1.531

^{a,b}Correspond to R_e values experimentally obtained in Ref. 6 for $X^1\Sigma^+$ and $B^1\Pi$ states, respectively.

for the $D^1\Pi$ state agree with their calculated counterparts within error bars, whereas the experimental data for the $B^1\Pi$ state are somewhat 15%–25% larger. The observed discrepancy exceeding the experimental error might be attributed to strong local spin-orbit coupling of the studied $B^1\Pi$ levels with near-lying rovibronic levels of the $b^3\Pi$ and $c^3\Sigma^+$ triplet states, see Fig. 3 of Ref. 7. An admixture of triplet electronic wave functions for the $B^1\Pi$ state is expected to be more pronounced than for the $D^1\Pi$ state because of much larger spin-orbit effects in the excited $\text{Rb}(5p)$ atom as compared to the $\text{Na}(3p)$ atom. Experimental data confirm the theoretical prediction of weak dipole moment dependence on rotational and vibrational quantum numbers, see Fig. 4.

It makes sense to mention that permanent electric dipole moments for the $B^1\Pi$ and $D^1\Pi$ states of NaRb are very close to the corresponding $\mu(R)$ -functions and $\mu(v')$ -values of the NaK molecule. Indeed, the experimental $\mu(v')$ -values of the nonperturbed $D^1\Pi$ levels of the NaK molecule vary from 5.9 D to 6.6 D for $v'=1-14$, see Table I of Ref. 1. Results of the most reliable *ab initio* finite-field MPPT $\mu(R)$ calculations for the NaK $B^1\Pi$ and $D^1\Pi$ states¹ are almost the same as in NaRb in the vicinity of the corresponding equilibrium distances.

It should be noted that any quantitative interpretation of the measured Λ -splittings is not possible at the present stage because of the lack of information about the relevant perturb-

ing states of NaRb. The *ab initio* calculation of the required potential curves and nonadiabatic matrix elements responsible for Λ -splitting of the $^1\Pi$ states is currently in progress.

ACKNOWLEDGMENTS

The Riga group participants have been supported by the Latvian Science Council (Grant No. 96.0323). O.N. is grateful for the support from Latvian Science Council Doctoral Studies Grant No. 44. The Moscow group participants have been supported by the Russian Fund of Basic Research under Grants No. 00-03-33004 and No. 00-03-32978. The authors would like to thank Dr. Monique Aubert-Frecon for placing the unpublished information on NaRb potentials to our disposal. The assistance of Olga Hrabrova in assigning the rovibronic levels, as well as of Janis Alnis and Arvids Zalcmans in fixing the experimental setup is gratefully acknowledged. We want to thank Dr. Janis Abolinsh for his efforts to improve the English style of the manuscript.

- ¹M. Tamanis, M. Auzinsh, I. Klincare, O. Nikolayeva, R. Ferber, E. A. Pazyuk, A. V. Stolyarov, and A. Zaitsevskii, *Phys. Rev. A* **58**, 1932 (1998).
- ²M. Tamanis, M. Auzinsh, I. Klincare, O. Nikolayeva, A. V. Stolyarov, and R. Ferber, *J. Chem. Phys.* **106**, 2195 (1997).
- ³H. Wang and W. C. Stwalley, *J. Chem. Phys.* **108**, 5767 (1998).
- ⁴H. Wang, P. L. Gould, and W. C. Stwalley, *Z. Phys. D: At., Mol. Clusters* **36**, 317 (1996).
- ⁵N. Takahashi and H. Katô, *J. Chem. Phys.* **75**, 4350 (1981).
- ⁶Y.-C. Wang, M. Kajitani, S. Kasahara, M. Baba, K. Ishikawa, and H. Katô, *J. Chem. Phys.* **95**, 6229 (1991).
- ⁷Y.-C. Wang, K. Matsubara, and H. Katô, *J. Chem. Phys.* **97**, 811 (1992).
- ⁸K. Matsubara, Y.-C. Wang, K. Ishikawa, M. Baba, A. J. McCaffery, and H. Katô, *J. Chem. Phys.* **99**, 5036 (1993).
- ⁹S. Kasahara, T. Ebi, M. Tanimura, H. Ikoma, K. Matsubara, M. Baba, and H. Katô, *J. Chem. Phys.* **105**, 1341 (1996).
- ¹⁰C. Amiot, O. Dulieu, and J. Vergés, *Phys. Rev. A* **83**, 2316 (1999).
- ¹¹P. J. Dagdigian and L. Wharton, *J. Chem. Phys.* **57**, 1487 (1972).
- ¹²H. Lefebvre-Brion and R. W. Field, *Perturbations in the Spectra of Diatomic Molecules* (Academic, New York, 1986).
- ¹³S. J. Silvers, T. H. Bergeman, and W. Klemperer, *J. Chem. Phys.* **52**, 4385 (1970).
- ¹⁴R. W. Field and T. H. Bergeman, *J. Chem. Phys.* **54**, 2936 (1971).
- ¹⁵M. Tamanis, M. Auzinsh, I. Klincare, O. Nikolayeva, R. Ferber, A. Zaitsevskii, E. A. Pazyuk, and A. V. Stolyarov, *J. Chem. Phys.* **109**, 6725 (1998).
- ¹⁶A. Zaitsevskii and J. P. Malrieu, *Theor. Chem. Acc.* **96**, 269 (1997).
- ¹⁷A. Zaitsevskii and R. Cimraglia, *Int. J. Quantum Chem.* **73**, 395 (1999).
- ¹⁸V. Kvasnicka, *Int. J. Quantum Chem.* **24**, 335 (1983).
- ¹⁹C. Angeli, R. Cimraglia, and M. Persico, *Theor. Chem. Acc.* **100**, 324 (1998).
- ²⁰E. A. Pazyuk, A. V. Stolyarov, A. Zaitsevskii, R. Ferber, P. Kowalczyk, and C. Teichteil, *Mol. Phys.* **96**, 955 (1999).
- ²¹L. F. Pacios and P. A. Christiansen, *J. Chem. Phys.* **82**, 2664 (1985).
- ²²L. A. LaJohn, P. A. Christiansen, R. B. Ross, T. Atashroo, and W. C. Ermler, *J. Chem. Phys.* **87**, 2812 (1987).
- ²³A. J. Sadlej and M. Urban, *J. Mol. Struct.: THEOCHEM* **234**, 147 (1991).